universität
innsbruck

Bachelor Thesis

The Three-Level Laser
as a Quantum Heat Engine

Markus Dannemüller

28. Juli 2021

Supervised by Univ.-Prof. Mag. Dr. Helmut Ritsch
and Dr. Laurin Ostermann
Institute for Theoretical Physics

Contents

1. Introduction

Thermodynamics is, in a broad sense, the study of heat and work. While attempts at understanding such concepts have existed since the antiquity, the French physicist Sadi Carnot is often regarded as one of the founders of thermodynamics. In a treatise published in 1824, he analysed the efficiency of heat engines, thereby introducing the famous Carnot engine: an idealised heat engine giving a theoretical upper bound to the efficiency, known as the Carnot limit [1]. The study of thermodynamics was initially focused on understanding steam engines, and was thus instrumental in the industrial revolution. But even nowadays, a plethora of heat engines are commonly used, ranging from various types of combustion engines to heat pumps and refrigeration devices [2].

Another, albeit more recent invention, which had far-reaching consequences for both industry and the sciences, is laser technology. One of the foundational ideas behind the laser is stimulated emission of photons [3]. While the laser would not be developed for decades, researchers, among them Albert Einstein, already discussed the three ways of light-matter-interaction (spontaneous emission, absorption, and stimulated emission) in the early twentieth century. The first experimental realisations of lasers succeeded in the 1950s, with Charles Townes often credited for the development of the first functioning prototype of a microwave laser, the so called 'maser', in 1954 [4].

In their 1959 paper [5], Scovil and Schulz-DuBois investigated whether a laser could not only be seen as a device transforming population inversion into coherent radiation, but also as a setup transforming a heat gradient into output power. Thus, they attempted a thermodynamic analysis of a single-atom laser and described it as a quantum heat engine [6]. This paper would lay the groundwork for the much later emerging theory of quantum thermodynamics, which attempts to find quantum mechanical, micro-scale analogues to the laws of classical thermodynamics.

Especially during the last decades, interest in the field of quantum thermodynamics has increased. Current research includes work on quantum heat engines and refrigerators, as well as on high-precision time-measuring devices and thermometry [7]. Researchers are also investigating fundamental connections between quantum thermodynamics and quantum information theory [8].

This work aims to introduce some fundamentals of quantum thermodynamics while analysing a simple model of a quantum heat engine: the three-level laser. First, some basics of lasers and heat engines are discussed. After an introduction to the model of a three-level laser coupled to thermal baths, a mathematical description based on open quantum systems is developed. Using the formalism of a Lindblad master equation, key thermodynamic observables are introduced within the context of quantum thermodynamics. Finally, the resulting equations are solved numerically, and the results are discussed.

2. Overview

The following sections introduce the ideas of lasers and heat engines, as well as the model of a three-level laser that is used throughout the remainder of this work.

2.1. Lasers

A laser consists of two primary elements: a gain medium and an optical resonator. The gain medium is a material with a radiative atomic transition between two atomic states $|g\rangle$ and $|e\rangle$. When an atom of the gain medium de-excites and releases a photon from this transition, it is captured inside the optical resonator and contributes to a cavity light field. However, the gain medium can also absorb photons of the same frequency; therefore, a laser can only function if there is population inversion. This means that the level $|e\rangle$ which is higher in energy must have a higher population than the lower energy level $|g\rangle$ [9].

However, considering two-level atoms is insufficient for a functioning laser: Even if the population was inverted initially, the populations of the two levels would equilibrate until on average no photons are added to the field. Thus, no long-lasting laser action would be possible. Any real laser, therefore, requires at least three atomic levels, with an additional auxiliary state added [10].

Population is constantly pumped into this auxiliary state from the lower state $|g\rangle$ and then de-excited into the upper state $|e\rangle$. If this de-excitation happens fast enough, the population in this auxiliary state will remain negligibly small. Most importantly, this pumping and de-excitation will lead to a non-equilibrium distribution of the population between the $|g\rangle$ and $|e\rangle$ states. The resulting constant population inversion now allows for long-lasting laser action [9].

As the photons are released from the gain medium via stimulated emission, they have characteristic properties which differ from those of other, classical light-sources such as thermal lamps. First, the radiation comes only from a single atomic transition at a given frequency, leading to a light field that is in many cases almost monochromatic. The finite width of the emitted frequency is due to natural broadening. This broadening is a direct consequence of the uncertainty principle for time and energy, and can therefore not be completely prevented. Second, the released photons also have fixed phase relations to each other; this property of laser light is known as coherence [9].

As a measure of coherence, the second-order time correlation function $g^{(2)}(0)$ can be used [9]. This function gives information on the correlation between single photon emissions. For thermal light-sources, $g^{(2)}(0) > 1$; this can be understood as photons 'bunching together', i.e. their emissions tend to be positively correlated. For coherent radiation, on the other hand, $g^{(2)}(0) = 1$, meaning that the emissions are completely uncorrelated. Thus, a value of $g^{(2)}(0) = 1$ can be seen as a measure of coherence.

A key idea of thermodynamics is the separation of a physical system into a subsystem, which is of primary interest, and an environment. It is then usually assumed that this environment is significantly larger than the subsystem. In this simplification, any impact of the subsystem on the internal state of the environment is assumed to be negligible. Thus, the subsystem cannot change the environment, but the environment can change the subsystem [11].

To allow for this influence of the environment on the subsystem, the partition between them typically enables one or more types of interaction: thermal (the exchange of energy), mechanical (the exchange of force), or chemical (the exchange of particles). The environment itself can then also be partitioned into multiple parts. These different parts may or may not have any interaction between each other [12].

A simple heat engine consists typically of a system partitioned into four parts: The subsystem, known as the work medium, and an environment split into a hot bath, a cold bath, and the work environment [11]. Such a heat engine can be visualised as a tricycle like in figure 1.
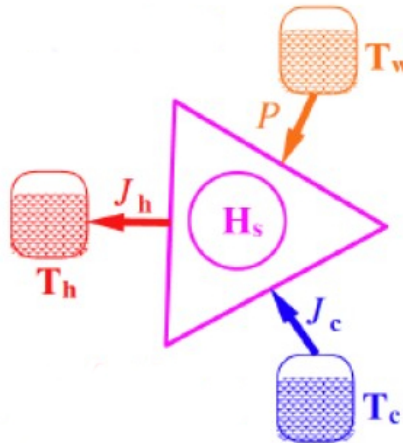
Figure 1: A simple heat engine in the form of a tricycle: The three parts of the environment are characterised by their respective temperatures T_i, and heat fluxes J_h and J_c as well as power P enter or leave the work medium in the centre. The model here depicts a cooling device, which can be seen as an inverse heat engine. Adapted from [13].

The hot bath is characterised by a temperature T_h above that of the work medium, and is thermally connected to the work medium. Hence, heat can flow from this hot bath into the work medium. Inside the work medium, some transformative process takes place. During this, part of the heat entering from the hot bath is rejected into the cold bath, which is described by a lower temperature T_c and is also thermally connected to

the work medium. Finally, the remaining energy leaves the work medium into the work environment not as heat, but as work. This could be achieved as a mechanical force, like a moving piston. So long as the heat gradient is sustained and the work process can be repeated, this leads to a transformation of a heat gradient to mechanical work [11].

A key figure of merit for heat engines is their efficiency in transforming heat gradients to power output. The efficiency η can be obtained as [11]

$$\eta = \frac{W}{Q_\mathrm{h}},\tag{1}$$

where W is the net work performed by the heat engine in one cycle, and Q_h is the heat entering the work medium during one cycle. Considering only an infinitesimally short time interval yields

$$\eta = \left|\frac{P}{\dot{Q}_\mathrm{h}}\right|.\tag{2}$$

Here, $P = \dot{W}$ denotes the net power leaving the system, and $\dot{Q}_\mathrm{h}$ the heat flux from the hot bath into the work medium. The absolute value is taken here to account for the signs of power and heat fluxes, for which there are different conventions. Throughout the remainder of this work, any flow into the subsystem will be considered positive, while a flow out of the subsystem will be negative.

2.3. Model

This section outlines the model of a three-level laser which is used throughout the remainder of this work. Natural units are used, where $\hbar = k_\mathrm{B} = 1$.

A single atom is used as the gain medium for the laser. This atom is described as a three-level system with a ground state $|g\rangle$ and two excited states $|l\rangle$ and $|p\rangle$. The atomic ground state $|g\rangle$ is chosen as the zero of energy; the excited states have energies ω_l and ω_p, respectively. Between these atomic levels, three different transitions are possible: the lasing transition between $|l\rangle$ and $|g\rangle$, the pumping transition between $|g\rangle$ and $|p\rangle$, and the cold transition between $|p\rangle$ and $|l\rangle$.

The atom is placed inside an optical resonator, the so called cavity. This cavity is constructed from mirrors which are positioned in such a way that light from the lasing transition with a frequency ω_l is resonant. The resulting cavity field then couples to the lasing transition.

Figure 2 shows a schematic view of the atom and cavity system. In section 3.1, the mathematical description of this system is developed.
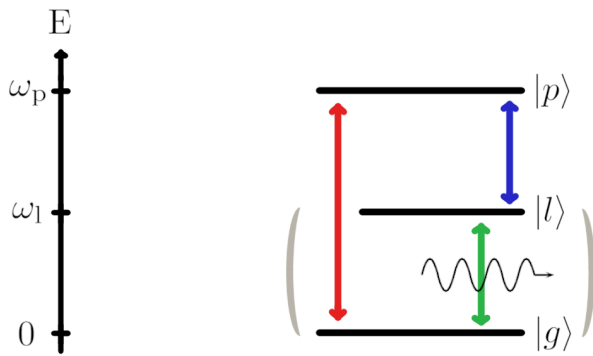
Figure 2: Schematic view of the atomic three-level system inside a cavity, with an energy scale on the left hand side. The three atomic states $|g\rangle$, $|l\rangle$, and $|p\rangle$ are connected via the lasing (green line), pumping (red line), and cold (blue line) transitions. The cavity mirrors are shown in grey, while the cavity field is indicated by a single photon.

In order to allow light to leave the cavity, one of the mirrors must have imperfections. This is modelled by a rate coefficient κ, which describes the rate at which photons from the cavity field leak out. The photons leak into the so-called work environment which surrounds the lasing system, i.e. the atom and cavity.

The pumping and cold transitions are driven by external radiation. This is modelled by introducing two additional parts to the environment: a hot and a cold bath. These are photonic baths at respective temperatures T_h and T_c with frequencies ω_p and $\omega_c := \omega_p - \omega_l$, whose photon number is given by Planck's law for thermal radiation

$$\bar{n}_{th}(\omega, T) = \left(\exp\left(\frac{\omega}{T}\right) - 1\right)^{-1},\tag{3}$$

where $\bar{n}_{th}$ denotes the expected number of photons at a given temperature T and frequency ω.

The interaction strength between these baths and the transitions is modelled via rate coefficients Γ_h and Γ_c for the hot and cold baths, respectively. In practice, such a source of radiation would not be monochromatic. However, a monochromatic photonic bath could be realised by using frequency filters that allow only resonant radiation to interact with the atomic system [5].

Figure 3 shows a schematic of the complete system consisting of the atom and the cavity, as well as the environment consisting of the two heat baths and the work environment; the work environment, i.e. the exterior world, is not shown explicitly. A mathematical description of the coupling processes between the atom-cavity-system and its environment is given in section 3.2.
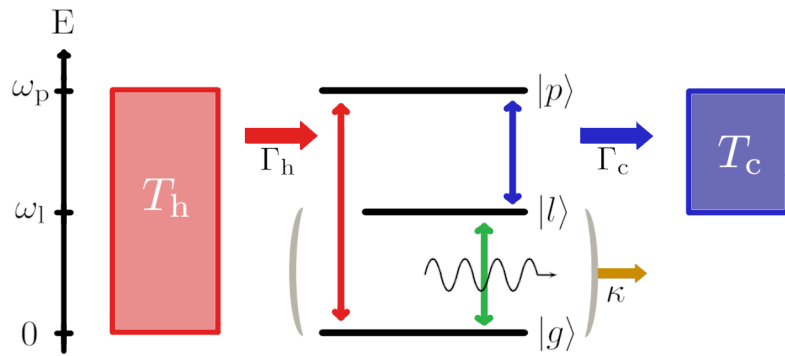
Figure 3: Schematic view of the atom-field system in contact with its environment, which consists of a hot and a cold photonic bath as well as a work environment (not shown explicitly). The interactions with the different parts of the environment are indicated using coloured arrows.

The functioning laser can then be understood in the following way: A photon from the hot bath leads to an atomic excitation, thereby pumping population from $|g\rangle$ to $|p\rangle$. This state then relaxes due to its coupling with the cold bath, which leads to an emission of a photon into the cold bath and a de-excitation of the atom from $|p\rangle$ to $|l\rangle$. Due to this pumping and cooling, a constant population inversion between $|g\rangle$ and $|l\rangle$ is achieved. The photons in the cavity field then lead to stimulated emission from $|l\rangle$ to $|g\rangle$, thereby adding coherent radiation to the cavity field. Due to the mirror imperfections, photons leak out of the cavity at a rate κ, which creates a beam of coherent laser light.

From a thermodynamic point of view, this system represents a tricycle as introduced in section 2.2. Energy is added into the work medium, i.e. the atomic system, in the form of heat from the hot bath. Then part of that energy is ejected into the cold bath, and the remaining energy is extracted as work in the form of radiation. These thermodynamic notions of heat and work are discussed in detail in section 3.3.

3. Mathematical Framework

The following sections introduce the mathematical description of the three-level model. First, the atom-field Hamiltonian is treated. After that, the dissipative parts of the model are described.

3.1. Closed System

As a first step towards a full description of the three-level laser, a mathematical model for the atom-field system is required. The atom-field system is composed of three relevant

parts: the atomic states, the cavity field, and the interaction between the two. The states which describe the atom-field system exist in a Hilbert space

$$\mathcal{H}_{\text{sys}} = \mathcal{H}_{\text{atom}} \otimes \mathcal{H}_{\text{field}}.$$

Operators acting only on the atomic or the field Hilbert space will be denoted in cursive, e.g. O being an operator acting on $\mathcal{H}_{\text{atom}}$. The corresponding operator acting on the complete Hilbert space $\mathcal{H}_{\text{sys}}$, which is obtained by tensorising with the appropriate identity element $\mathbb{1}_i$, will be denoted in bold face, e.g.

$$\boldsymbol{O} := O \otimes \mathbb{1}_{\text{field}}.$$

A Hamiltonian describing the entire atom-field system will be of the form

$$\boldsymbol{H}_{\text{sys}} = \boldsymbol{H}_{\text{atom}} + \boldsymbol{H}_{\text{field}} + \boldsymbol{H}_{\text{int}}, \tag{4}$$

where $\boldsymbol{H}_{\text{atom}}$ describes the atomic three-level system, $\boldsymbol{H}_{\text{field}}$ the cavity field, and $\boldsymbol{H}_{\text{int}}$ the atom-field interaction. In the following, all three parts of the system Hamiltonian will be treated separately.

First, the atomic Hamiltonian is treated. The atom can be described as a three-level system with a Hilbert space $\mathcal{H}_{\text{atom}} \cong \mathbb{C}^3$. By simply taking the projection operators $|i\rangle\langle i|$ onto each of the atomic states and multiplying them with their respective frequencies, the atomic Hamiltonian is found to be

$$H_{\text{atom}} = \omega_{\text{l}}|l\rangle\langle l| + \omega_{\text{p}}|p\rangle\langle p|. \tag{5}$$

The ground state vanishes in the Hamiltonian, as it was chosen as the zero of energy.

Next, the field Hamiltonian is covered. The cavity field can be understood as a quantum harmonic oscillator whose energy levels are shifted such that the field ground state coincides with the zero of energy. The Fock states $\{|n\rangle\}_{n \in \mathbb{N}_0}$ can be used as a basis for its infinite-dimensional Hilbert space $\mathcal{H}_{\text{field}}$. These represent n excitations in the oscillator, which are interpreted as photons in the light field [14].

Using the formalism of second quantisation, the creation operator $a^\dagger$ and the annihilation operator a can be introduced, which satisfy

$$a^\dagger|n\rangle = \sqrt{n+1}\,|n+1\rangle,$$
$$a|n\rangle = \sqrt{n}\,|n-1\rangle,$$
$$a|0\rangle = 0,$$
$$[a, a^\dagger] = \mathbb{1}_{\text{field}}.$$

As can be seen from these relations, the number operator $a^\dagger a$ returns the number of excitations as an eigenvalue when acting on a Fock state $|n\rangle$.

The total energy of the field is simply the number of photons times the energy per photon. As each photon has an energy ω_l, the Hamiltonian for the cavity field can be obtained as

$$\boldsymbol{H}_\textbf{field} = \omega_\mathrm{l}\, \boldsymbol{a}^\dagger \boldsymbol{a}. \tag{6}$$

Lastly, the interaction term between the atom and field is treated. Assuming that the cavity field only couples with the atomic transition between $|g\rangle$ and $|l\rangle$, this interaction is equivalent to that of a two-level system interacting with a harmonic oscillator. A standard approach to describing such a form of interaction is the Jaynes-Cummings model. The following derivation approximately follows [15].

The atom's reduced two-state system can be understood as an electric dipole. This can be treated in analogy to the classical case, where one obtains for an electric dipole with dipole moment $\vec{D}_\mathrm{c}$ in an external electric field $\vec{E}_\mathrm{c}$ an interaction energy of $E_\mathrm{dipole} = -\vec{D}_\mathrm{c} \cdot \vec{E}_\mathrm{c}$. Using the formalism of canonical quantisation, the dipole moment is replaced by the atomic dipole operator $\boldsymbol{D}$. By introducing the atomic raising and lowering operators

$$\sigma_\mathrm{l}^+ := |l\rangle\langle g|,$$
$$\sigma_\mathrm{l}^- := |g\rangle\langle l|,$$

the dipole operator can be written as

$$\boldsymbol{D} = d\left(\boldsymbol{\sigma_\mathrm{l}^+} + \boldsymbol{\sigma_\mathrm{l}^-}\right).$$

Here, d is the dipole operator matrix element

$$d = \langle g|\boldsymbol{D}|l\rangle = \langle l|\boldsymbol{D}|g\rangle.$$

In order to obtain a fully quantum treatment of this dipole interaction, the electric field must also be quantised. Starting from the Maxwell equations in vacuum and again using the creation and annihilation operators $a^\dagger$ and a, the electric field operator can be expressed as

$$\boldsymbol{E} = E_0\left(\boldsymbol{a} + \boldsymbol{a}^\dagger\right),$$

where E_0 is the magnitude of the electric field. For brevity, a more detailed derivation of this quantised electric field is omitted here.

The interaction Hamiltonian will then be of the form $H_{\text{int}} = DE$. Next, a transformation from the Schrödinger picture into the interaction picture with respect to $H_0 := H_{\text{atom}} + H_{\text{field}}$ is performed. This transforms an operator O according to

$$\tilde{O} = e^{itH_0} O e^{-itH_0},$$

where a tilde now represents an operator in its interaction picture representation.

For example, the atomic upwards transition operator σ_1^+ transforms as

$$
\begin{aligned}
\tilde{\sigma}_1^+ &= e^{itH_{\text{atom}}} \sigma_1^+ e^{-itH_{\text{atom}}} \\
&= \left(e^{itH_{\text{atom}}} |l\rangle \right) \left(e^{itH_{\text{atom}}} |g\rangle \right)^\dagger \\
&= e^{it\omega_l} \sigma_1^+,
\end{aligned}
$$

where the first equality follows from $\left[H_{\text{field}}, \sigma_1^+ \right] = 0$, as these operators only have non-trivial actions on different Hilbert spaces. Similarly, the remaining operators transform as

$$
\begin{aligned}
\tilde{\sigma}_1^- &= e^{-it\omega_l} \sigma_1^-, \\
\tilde{a}^\dagger &= e^{it\omega_l} a^\dagger, \\
\tilde{a} &= e^{-it\omega_l} a.
\end{aligned}
$$

In the interaction picture, the interaction Hamiltonian is then given by

$$dE_0 \left(\tilde{\sigma}_1^+ \tilde{a}^\dagger + \tilde{\sigma}_1^- \tilde{a}^\dagger + \tilde{\sigma}_1^+ \tilde{a} + \tilde{\sigma}_1^- \tilde{a} \right).$$

The terms $\tilde{\sigma}_1^- \tilde{a}^\dagger$ and $\tilde{\sigma}_1^+ \tilde{a}$ are time-independent, as the exponential prefactors cancel. The two remaining terms, on the other hand, are time-dependent: $\tilde{\sigma}_1^+ \tilde{a}^\dagger \sim e^{2i\omega_l t}$ and $\tilde{\sigma}_1^- \tilde{a} \sim e^{-2i\omega_l t}$. These two fast-oscillating terms are ignored in what is called the rotating-wave-approximation, as they are assumed to average out on the relevant time-scale of the system. Using this approximation and transforming back into the Schrödinger picture, the interaction term simplifies to

$$H_{\text{int}} = g \left(\sigma_1^- a^\dagger + \sigma_1^+ a \right), \tag{7}$$

where $g := dE_0$ is a constant describing the interaction strength.

Finally, putting equations (5), (6), and (7) together, the total Hamiltonian for the atom-field system is obtained as

$$\boldsymbol{H_{\text{sys}}} = \omega_{\text{l}}|\boldsymbol{l}\rangle\langle\boldsymbol{l}| + \omega_{\text{p}}|\boldsymbol{p}\rangle\langle\boldsymbol{p}| + \omega_{\text{l}}\boldsymbol{a}^\dagger\boldsymbol{a} + g\left(\boldsymbol{\sigma_{\text{l}}^-}\boldsymbol{a}^\dagger + \boldsymbol{\sigma_{\text{l}}^+}\boldsymbol{a}\right), \tag{8}$$

with the projection operators

$$|\boldsymbol{i}\rangle\langle\boldsymbol{i}| := |i\rangle\langle i| \otimes \mathbb{1}_{\text{field}}.$$

Using this Hamiltonian, the atom-field system alone could be fully described. What is missing so far, however, are terms describing the interaction of this atom-field system with its environments – the hot and cold baths as well as the work environment. These are discussed in the following section.

3.2. Open System

The states of the total system exist in a Hilbert space

$$\mathcal{H}_{\text{tot}} = \mathcal{H}_{\text{sys}} \otimes \mathcal{H}_{\text{env}},$$

where $\mathcal{H}_{\text{env}}$ describes all parts of the environment. An arbitrary state on this total Hilbert space can be described by a density operator $\rho_{\text{tot}}(t)$. Encoded in this density operator is a complete description of the total system's state at a given time t. Therefore, it contains a detailed description of the internal state of both the hot and cold heat baths, and of the work environment.

However, the part of the system whose description is of physical interest is only the atom-field system; the internal state of the environment is of lesser importance. This atom-field state ρ can be obtained by tracing out the environment degrees of freedom:

$$\rho(t) = \text{Tr}_{\text{env}}\left(\rho_{\text{tot}}(t)\right),$$

where Tr_{env} denotes the partial trace over the environment.

In order to now obtain the time evolution of an initial state $\rho(0)$, a similar approach to the prior section could be taken, where now a Hamiltonian describing the environment could be derived. Following this, unitary time evolution would lead to the desired state of the system at a given time t.

Instead of this explicit description of the environment, however, an implicit description can also be used: Rather than describing the total system in terms of a total Hamiltonian and then tracing out the 'uninteresting' environment, only the atom-field system is described using the Hamiltonian of equation (8), while the influence of the environment is implicitly described via some interaction terms. These interaction terms represent energy flowing into or out of the atom-field system. However, this means that energy is not preserved in the atom-field system, and therefore the resulting time evolution will be non-unitary.

Using this approach, the von-Neumann equation

$$\dot{\rho} = -i\left[\boldsymbol{H}_{\mathbf{sys}}, \rho\right]$$

is no longer sufficient to describe the time evolution of the system, as it neglects the influence of the environment on the system dynamics. To account for this, a new dissipative term is added to the time-evolution, yielding

$$\dot{\rho} = -i\left[\boldsymbol{H}_{\mathbf{sys}}, \rho\right] + \frac{1}{2}\sum_k \left(2\boldsymbol{J_k}\rho\boldsymbol{J_k}^\dagger - \left\{\boldsymbol{J_k}^\dagger\boldsymbol{J_k}, \rho\right\}\right), \tag{9}$$

where $\{\cdot,\cdot\}$ is the anti-commutator and $\{J_k\}$ are a set of so-called jump operators describing the various dissipative interactions between system and environment. Equation (9) is known as the master equation in Lindblad form and gives a full description of the time-development of a system that is subject to a Hamiltonian as well as dissipative effects. A full derivation of the master equation can be found for example in [15] or in [16].

However, before the master equation can be used to describe the dynamics of the three-level laser, the various jump operators J_k need to be identified first.

The total system includes three parts where a dissipative interaction between the atom-field system and the environment occurs: the interaction at the pumping transition and the hot bath, that at the cold transition and the cold bath, and the leaking of photons from the cavity into the work environment. In the following, each of these is described separately.

When considering only the pumping transition and the hot photonic bath, the atom can effectively be seen as a two-level system with states $|g\rangle$ and $|p\rangle$ and only the single transition between them. This is therefore equivalent to a two-level atom decaying in a thermal field, and only two different dissipative processes are possible: Either the atom absorbs a photon from the hot bath and is excited from $|g\rangle$ to $|p\rangle$, or it emits a photon while decaying from $|p\rangle$ to $|g\rangle$.

As shown for example in [15], the resulting jump operators are given by

$$J_{\mathrm{h},1} = \sqrt{\Gamma_{\mathrm{h}}\left(1 + \bar{n}_{\mathrm{th,h}}\right)}\ \sigma_{\mathrm{p}}^-$$
$$J_{\mathrm{h},2} = \sqrt{\Gamma_{\mathrm{h}}\bar{n}_{\mathrm{th,h}}}\ \sigma_{\mathrm{p}}^+,$$

where Γ_{h} is a rate coefficient describing the interaction strength and $\bar{n}_{\mathrm{th,h}}$ is the expected number of thermal photons in the hot bath according to equation (3) for a temperature T_{h} and a frequency ω_{p}. $\sigma_{\mathrm{p}}^- := |g\rangle\langle p|$ is the lowering operator for the pumping transition, and $\sigma_{\mathrm{p}}^+ := |p\rangle\langle g|$ is the raising operator.

How can these jump operators be interpreted? For the downwards transition, two additive terms appear under the square root. The 1-term represents spontaneous decay,

while the $\bar{n}_{\mathrm{th,h}}$-term represents stimulated emission. For the upwards transition, only the $\bar{n}_{\mathrm{th,h}}$-term appears, which represents an absorption process. Clearly, there can be no 'spontaneous excitation' without absorbing a photon; therefore, the upwards transition lacks the 1-term [15].

The jump operators for the cold transition are obtained analogously:

$$J_{\mathrm{c,1}} = \sqrt{\Gamma_{\mathrm{c}}\left(1 + \bar{n}_{\mathrm{th,c}}\right)} \; \sigma_{\mathrm{c}}^{-}$$
$$J_{\mathrm{c,2}} = \sqrt{\Gamma_{\mathrm{c}}\bar{n}_{\mathrm{th,c}}} \; \sigma_{\mathrm{c}}^{+}.$$

Here, Γ_{c} is the rate coefficient of the cold bath interaction, $\bar{n}_{\mathrm{th,c}}$ is the expected number of photons at temperature T_{c} and the cold transition frequency $\omega_{\mathrm{c}} := \omega_{\mathrm{p}} - \omega_{\mathrm{l}}$, and $\sigma_{\mathrm{c}}^{-} := |l\rangle\langle p|$, $\sigma_{\mathrm{c}}^{+} := |p\rangle\langle l|$ are the transition operators for the cold transition.

Finally, a jump operator for the photons leaking from the cavity field into the work environment is needed. Photons are only allowed to leave the cavity, therefore a single jump operator suffices. This operator is given by

$$J_{\mathrm{cav}} = \sqrt{\kappa} \; a,$$

where a is again the field annihilation operator, representing the removal of a single photon from the cavity field.

With this, all required jump operators have been described. Using them with the master equation gives the time evolution of the three-level laser. However, before it is possible to analyse the system as a heat engine, thermodynamic observables must be introduced.

3.3. Quantum Heat Engine

As discussed in section 2.2, the efficiency is a key figure of merit for heat engines. In order to calculate it, however, some notions of power and heat flux are required. Therefore, the aim of this section is to derive a quantum mechanical analogue to the first law of thermodynamics.

Working in the Schrödinger picture so far, the states described by density operators were time-dependent, while observables were time-independent. At this point, however, it is convenient to switch into the Heisenberg picture, where now observables are time-dependent and states time-independent.

Starting from the master equation, it can be shown [13] that the time-evolution of an observable $\boldsymbol{O}$ in the Heisenberg picture is given by

$$\dot{\boldsymbol{O}} = i\left[\boldsymbol{H}_{\mathbf{sys}}, \boldsymbol{O}\right] + \frac{1}{2}\sum_{k}\left(2\boldsymbol{J}_{\boldsymbol{k}}^{\dagger}\boldsymbol{O}\boldsymbol{J}_{\boldsymbol{k}} - \left\{\boldsymbol{J}_{\boldsymbol{k}}^{\dagger}\boldsymbol{J}_{\boldsymbol{k}}, \boldsymbol{O}\right\}\right) \equiv i\left[\boldsymbol{H}_{\mathbf{sys}}, \boldsymbol{O}\right] + \frac{1}{2}\sum_{k}\mathcal{D}_{k}[\boldsymbol{O}], \quad (10)$$

where again k runs over all dissipative terms in the master equation. The newly introduced short-hand $\mathcal{D}_k[\boldsymbol{O}]$ is sometimes referred to as the k-th 'dissipator' acting on an observable $\boldsymbol{O}$.

As the first law of thermodynamics can be seen as a balance equation for energy, it might be interesting to consider the change in energy of the system as it develops according to the master equation. Replacing $\boldsymbol{O}$ with $\boldsymbol{H}_{\mathbf{sys}}$ in equation (10) yields

$$\dot{\boldsymbol{H}}_{\mathbf{sys}} = \frac{1}{2}\sum_k \mathcal{D}_k[\boldsymbol{H}_{\mathbf{sys}}],$$

where the commutator vanishes as $\boldsymbol{H}_{\mathbf{sys}}$ of course commutes with itself.

Taking expectation values on both sides of this equation, and defining $\dot{E} := \langle \dot{\boldsymbol{H}}_{\mathbf{sys}}\rangle$, one obtains

$$\dot{E} = \frac{1}{2}\sum_k \langle \mathcal{D}_k[\boldsymbol{H}_{\mathbf{sys}}]\rangle.$$

Now, the heat flux from the hot and cold baths, respectively, is identified as

$$\dot{Q}_{\mathrm{h(c)}} := \frac{1}{2}\langle \mathcal{D}_{\mathrm{h(c)},1}[\boldsymbol{H}_{\mathbf{sys}}] + \mathcal{D}_{\mathrm{h(c)},2}[\boldsymbol{H}_{\mathbf{sys}}]\rangle,$$

and the power is identified as

$$P := \frac{1}{2}\langle \mathcal{D}_{\mathrm{cav}}[\boldsymbol{H}_{\mathbf{sys}}]\rangle.$$

It should be noted that in these identifications, one key assumption was made: that the light leaking from the cavity mirrors is pure power and thus has zero entropy associated with it. This could be understood as the work environment being arbitrarily hot, i.e. $T_{\mathrm{w}} \to \infty$ [17]. According to Clausius' formulation of the second law of thermodynamics, heat never flows spontaneously from a cold body to a hot one. Therefore, all the energy flowing into the work environment must be pure power. For the purposes of this work, it is assumed that this identification is justified.

With these identifications, one obtains

$$\dot{E} = \dot{Q}_{\mathrm{h}} + \dot{Q}_{\mathrm{c}} + P, \tag{11}$$

which is a time-derivative of the first law of thermodynamics. Using these new quantum-thermodynamic observables of power and heat flux, the efficiency η is defined analogously to the classical thermodynamic case of equation (2) via

$$\eta := \left|\frac{P}{\dot{Q}_{\mathrm{h}}}\right|, \tag{12}$$

where the absolute value was taken to ensure a positive sign of the efficiency, as power flowing out of the system is a negative quantity, while heat flowing into the system is positive.

Another key quantity in thermodynamics is the entropy S. In this quantum-thermodynamic case, the entropy is taken to be the von-Neumann entropy S_{VN}, defined as

$$S_{\text{VN}} := -\text{Tr}\left(\rho \log\left(\rho\right)\right). \tag{13}$$

Meaningful definitions of the second and third laws of thermodynamics within the context of quantum-thermodynamics are also possible (see for example [13]). However, these go beyond the scope of this work and are therefore not included here.

Having now developed the necessary quantum-thermodynamic observables which are required to analyse the model as a heat engine, the following section introduces the approach to the numerical solution of the model and discusses the obtained results.

4. Results

The model of the three-level laser, which was developed in the prior sections, was solved numerically using the 'julia' programming language and, in particular, the QuantumOptics.jl package [18]. Unless explicitly stated otherwise, the following parameters were used for the simulations: $\omega_{\text{l}} = 1000\kappa$, $g = 50\kappa$, $\Gamma_{\text{h}} = \Gamma_{\text{c}} = 400\kappa$, $\omega_{\text{p}}/T_{\text{h}} = 1.5$, $\omega_{\text{c}}/T_{\text{c}} = 5$ and $\omega_{\text{p}} = 1.5\omega_{\text{l}}$.

In the following, the results of the numerical simulation are discussed. This discussion is roughly structured in two parts: First, the system is analysed with regards to its functionality as a laser. Second, a closer look is taken at the thermodynamic observables.

4.1. Analysis of the Laser

The left hand side of figure 4 shows a plot of the populations of the atomic levels as a function of time, scaled in units of Γ_{h}. As can be seen, the population in the pumping state $|p\rangle$ stays low throughout the entire time development, and reaches a steady state almost instantaneously. After some initial fluctuations, the populations in $|l\rangle$ and $|g\rangle$ also approach a steady state. Most importantly, the population of $|l\rangle$ in the steady state remains slightly larger than that of $|g\rangle$. This population inversion, as discussed in section 2.1, is a necessary prerequisite for sustained stimulated emission of photons into the cavity field.

16
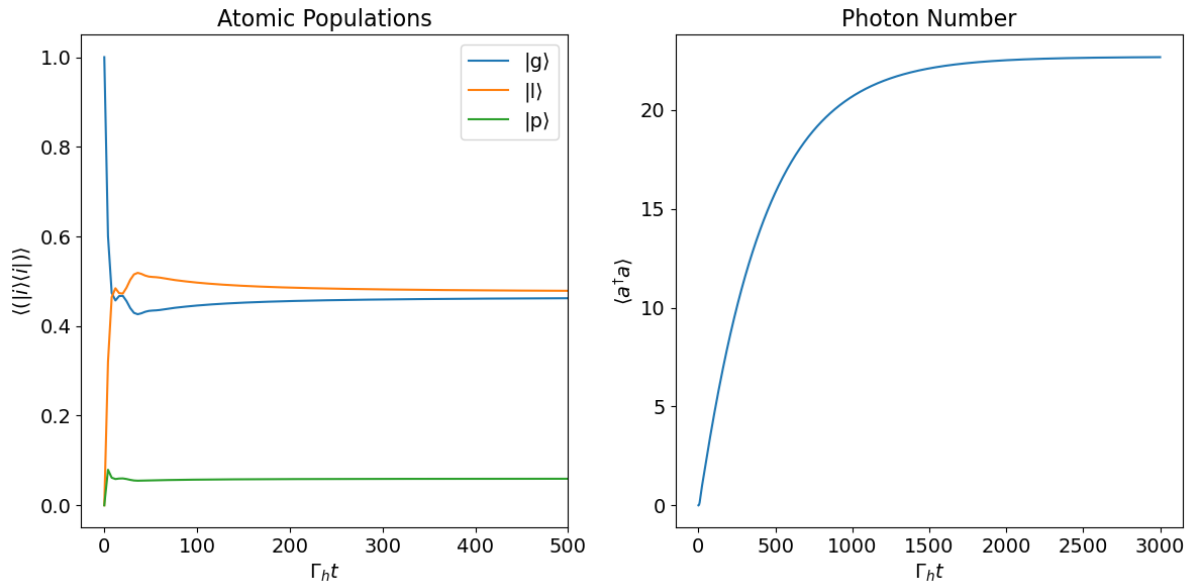
Figure 4: Left: atomic populations as a function of time. Right: expected number of photons in the cavity field.

The right hand side of figure 4 shows the time development of the average number of photons in the cavity field, given by the expectation value $\langle a^\dagger a \rangle$ of the number operator. Initially, the cavity field is prepared in a vacuum state. As the pumping and cooling processes lead to population inversion of the $|l\rangle$ and $|g\rangle$ levels, an increasing number of photons is emitted into the cavity field. Eventually, the field also reaches a steady state. This can be understood as a point when the number of photons added to the field per unit of time is equal to the number of photons leaking from the cavity mirror in the same time interval.

On the left, figure 5 shows a histogram of the photon number distribution in the steady state (blue bars). In order to more easily compare this to the theoretically expected Poissonian distribution, an ideal distribution was added (orange dots). As can be seen, the observed photon statistics fit the expectation very well.
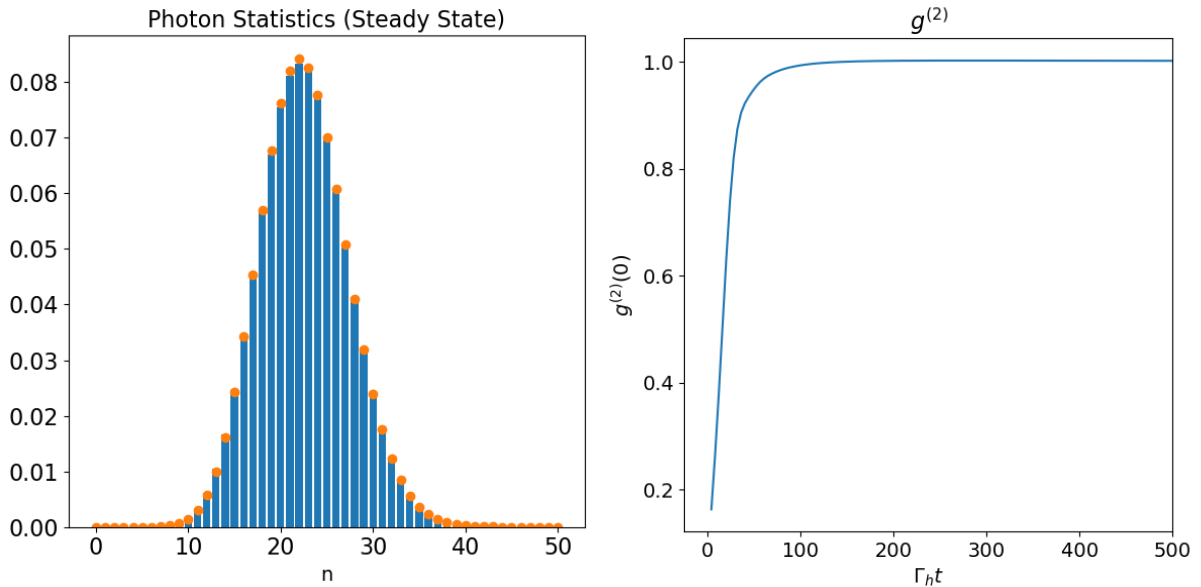
Figure 5: Left: a histogram of the steady state photon distribution, with an ideal Poissonian distribution in orange. Right: g^2 as a function of time.

Finally, the radiation field emitted from a laser is expected to be coherent. As discussed in section 2.1, the two-time correlation function $g^{(2)}(0)$ can be seen as a measure of coherence. Using the previously introduced field creation and annihilation operators, this function can be expressed as [9]

$$g^{(2)}(0) = \frac{\langle a^\dagger a^\dagger a a \rangle}{\langle a^\dagger a \rangle^2}. \tag{14}$$

It is plotted against time on the right in figure 5.

Initially, there are no emission processes, and therefore there is also no correlation between them. Afterwards, the value of $g^{(2)}$ almost instantly reaches its steady state of 1, implying a coherent light field in the cavity.

All of this together shows that the laser in its steady state is functioning as expected: The $|l\rangle$ state has higher population than the $|g\rangle$ state, thereby allowing for stimulated emission. The cavity field contains coherent radiation, which leaks out of the laser system, and the photon statistics obeys the characteristic Poissonian distribution.

It might also be interesting to analyse the impact of the strength of pumping on the laser. To look into this, the hot bath temperature T_{h} is varied.

As expected, for a very low heat gradient $T_{\text{h}} \lesssim 5T_{\text{c}}$, the pumping is too weak and no population inversion is obtained. More interestingly, the lasing action also breaks down for very strong pumping $T_{\text{h}} \gg T_{\text{c}}$. In figure 6, the steady state photon statistics are shown for different values of T_{h}. For $\omega_{\text{p}}/T_{\text{h}} = 0.15$, the distribution already deviates

strongly from a Poissonian distribution. For an even higher temperature, $\omega_{\mathrm{p}}/T_{\mathrm{h}} = 0.05$, the distribution is very close to a Bose-Einstein distribution

$$P(n) = \frac{1}{\langle n \rangle + 1} \left(\frac{\langle n \rangle}{\langle n \rangle + 1} \right)^n \tag{15}$$

for $\langle n \rangle = 4$. Such a distribution is characteristic of thermal light [19].

This behaviour, while unintuitive, fits the observations by Li et al [20]. As they argue in their paper, a higher temperature T_{h} does not only increase the pumping, but it also increases the atomic decay rate, which ultimately leads to a break down of the laser system for extreme values of T_{h}. This effect could be avoided by using a four-level laser model instead.
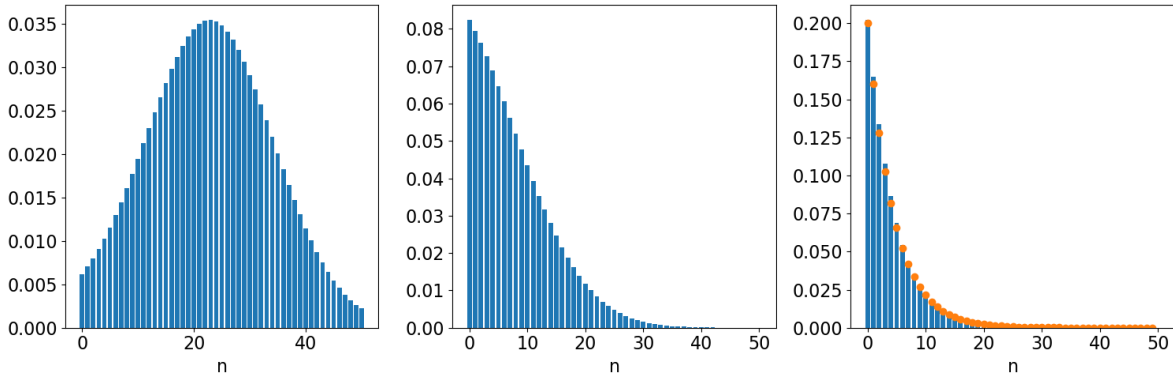
Figure 6: Steady state photon statistics for different values of T_{h}: On the left, $\omega_{\mathrm{p}}/T_{\mathrm{h}} = 0.15$; in the centre, $\omega_{\mathrm{p}}/T_{\mathrm{h}} = 0.06$; and on the right, $\omega_{\mathrm{p}}/T_{\mathrm{h}} = 0.05$. In the right-hand plot, a Bose-Einstein-distribution is shown in orange.

4.2. Analysis of the Heat Engine

Figure 7 shows the time-development of the hot and cold heat fluxes (left hand side) as well as that of the power (right hand side). As expected, the hot heat flux is positive, as it goes into the system, while both the cold heat flux and the power are negative. The power develops similarly to the photon number in the cavity. This is to be expected: The more photons there are in the cavity field, the higher the number that escape the cavity at the fixed rate κ.

After some initial oscillation, the heat fluxes almost instantaneously reach their steady state values. The power, just like the photon number before, approaches its steady state much more slowly. It can also be seen that the magnitude of cold heat flux and power together equal the magnitude of the hot heat flux in the steady state. This has to be the case, as in the steady state the energy of the system can no longer change.
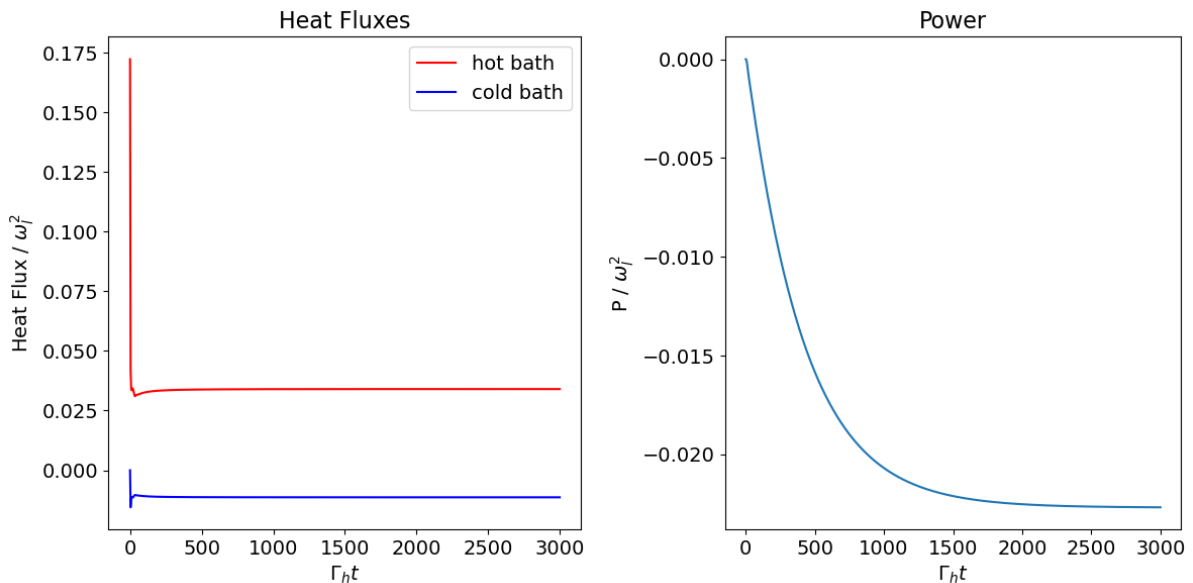
Figure 7: Time development of the heat fluxes (left) and of the power (right).

Using the heat fluxes and power shown above, the efficiency was calculated according to equation (12). Its time development is shown in figure 8.

As the heat fluxes have almost no time development except at the very beginning, the efficiency curve follows the power curve closely. For the chosen parameters, it reaches a value of $\frac{2}{3}$ in its steady state. This is well below the Carnot limit of $\frac{9}{10}$. As already shown by Scovil and Schulz-DuBois in their original paper [5], the steady state efficiency fulfils

$$\eta_{\mathrm{SS}} = \frac{\omega_{\mathrm{l}}}{\omega_{\mathrm{p}}}.$$

Even without any rigorous mathematical approach, this result is immediately evident when thinking of the three-level laser as a thermodynamic tricycle: In the steady state, the energy of the system cannot change. Therefore, for every excitation coming into the system from the hot bath (as a heat flux with magnitude ω_{p}), exactly one excitation has to leave the system into the cold bath, and one excitation has to leave into the work environment as a photon (as power with magnitude ω_{l}). Therefore, the ratio of power to heat flux must approach the ratio of the lasing to the pumping frequency in steady state.
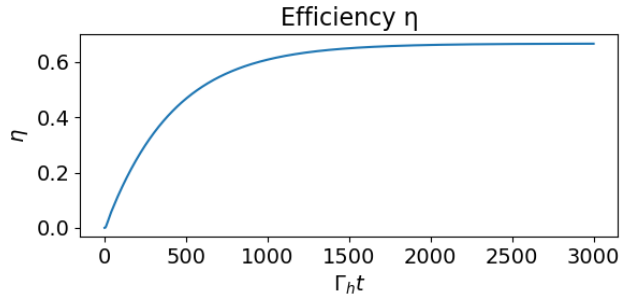
Figure 8: Time development of the efficiency η, as defined in equation (12).

So far, the focus was on the time development and the resulting steady state for a single set of parameters only. For the following steady state analysis, both bath temperatures T_h and T_c are varied. Figure 9 shows the heat fluxes, the magnitude of the power, and the von-Neumann entropy as functions of these control parameters, both scaled in units of the lasing frequency ω_l.

It can be clearly seen that the magnitudes of both heat fluxes and power show the same qualitative behaviour: For increasing temperature gradients $T_\mathrm{h} - T_\mathrm{c}$, they also increase, while for decreasing gradients, they decrease. The range of parameters chosen here all lead to a functioning laser; for even lower temperature gradients, the laser begins to break down as no population inversion is achieved – instead of coherent light, only thermal radiation is emitted. The steady-state entropy, on the other hand, shows more complex behaviour: For any given value of T_c, there is a local maximum with regards to T_h, and vice versa.

The behaviour of the hot heat flux and the power also clearly shows that their ratio remains fixed in the steady state for any of the chosen parameter combinations. This supports the earlier observation that the steady state efficiency should depend only on the energy levels of the atom, and not on other control parameters, such as the temperature of the baths.
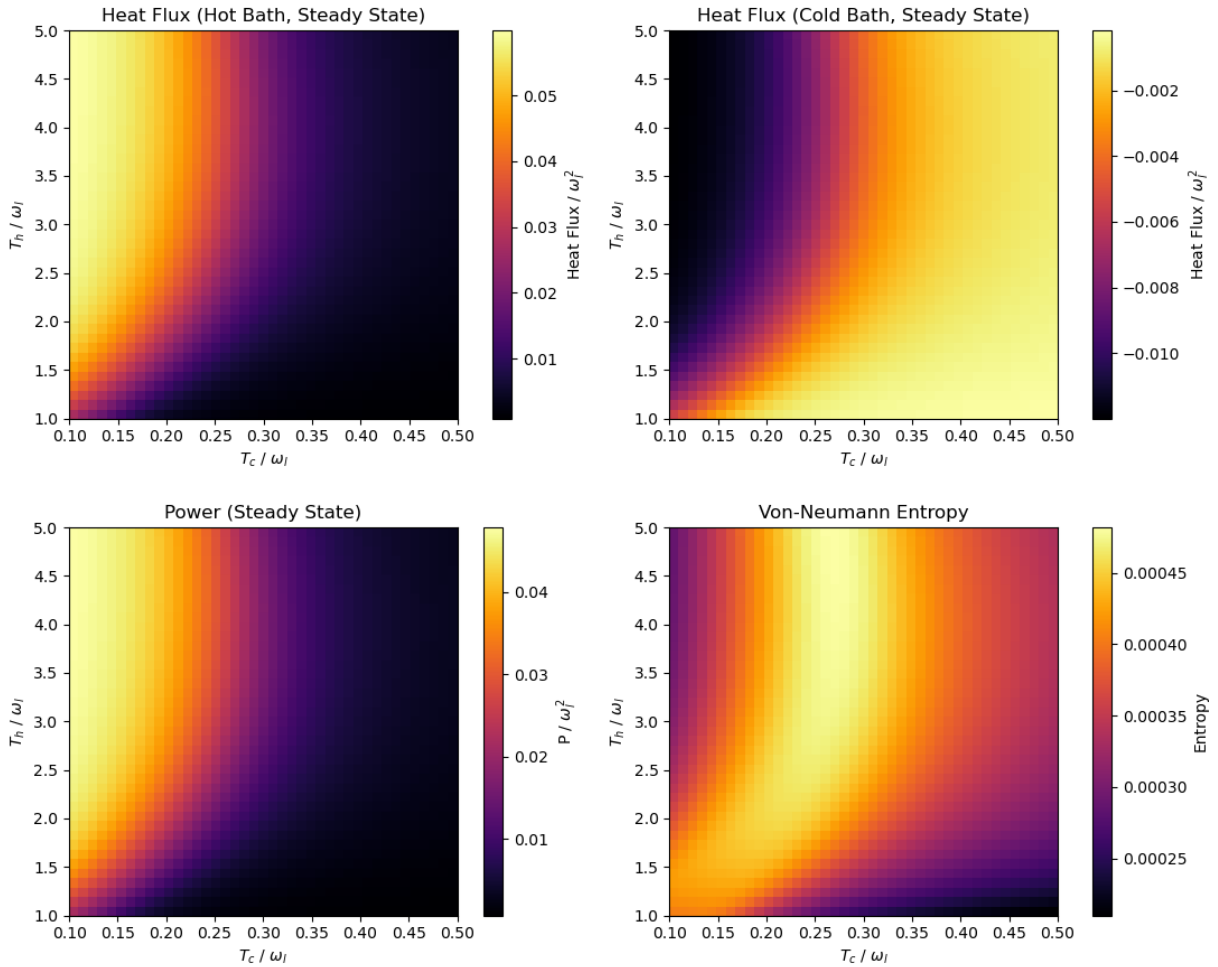
Figure 9: Steady state heat fluxes (top row), magnitude of the power (bottom left), and entropy (bottom right) as functions of the control parameters T_{h} and T_{c}.

5. Conclusion

In this work, a single-atom three-level laser was analysed as a model of a quantum mechanical heat engine. While the atom-field-system was described explicitly using a Hamiltonian, the interaction with two heat baths and the work environment was described via dissipative processes. Using the formalism of open quantum systems, a master equation was used to obtain the system's time development. In order to analyse the heat engine, some key quantum-thermodynamic observables were introduced.

Numerical simulations of the model were done using the 'julia' programming language. The system was found to be a functioning laser in its steady state for a range of different bath temperatures, as it converted a heat gradient between the baths into population inversion, finally resulting in coherent radiation output. Furthermore, the cavity field's photon statistics matched the expected Poissonian distribution.

It was also shown that the three-level laser not only breaks down for weak pumping, but also for extremely strong pumping, i.e. at very high temperatures of the hot bath. This is in agreement with a recent publication by Li et al [20].

The three-level laser was also found to be a functioning thermodynamic tricycle: A heat flux flowing into the system from the hot bath was in part rejected into the cold bath, while the remaining energy left the system as a coherent radiation field. This radiation was interpreted as the power output of the system.

Interestingly, it was seen that the steady state efficiency of the heat engine is independent from the bath temperatures, at least for heat gradients which allow for population inversion. Instead, the efficiency depends only on the ratio of the pumping and lasing frequencies, in full agreement with the 1959 paper by Scovil and Schulz-DuBois [5].

In the future, it might be interesting to also consider a four-level laser and compare it to the three-level model presented here. More attention might also be given to the question whether the identifications of heat fluxes and power, as performed in this work, are justified.

References

[1] G. S. Girolami. "A brief history of thermodynamics, as illustrated by books and people". *Journal of Chemical & Engineering Data*. **65**(2). 2019, pp. 298–311.

[2] C. R. Ferguson and A. T. Kirkpatrick. *Internal combustion engines: applied thermosciences*. John Wiley & Sons, 2015.

[3] B. E. A. Saleh and M. C. Teich. *Fundamentals of photonics*. eng. 3rd ed. Wiley series in pure and applied optics. Newark: Wiley, 2019. ISBN: 1119506875.

[4] A. J. Gross and T. R. Herrmann. "History of lasers". *World journal of urology*. **25**(3). 2007, pp. 217–220.

[5] H. E. D. Scovil and E. O. Schulz-DuBois. "Three-Level Masers as Heat Engines". *Phys. Rev. Lett.* **2** *. 1959 6, pp. 262–263.
DOI: 10.1103/PhysRevLett.2.262.

[6] R. Alicki and R. Kosloff. "Introduction to quantum thermodynamics: History and prospects". *Thermodynamics in the Quantum Regime*. Springer, 2018, pp. 1–33.

[7] P. P. Hofer, M. Perarnau-Llobet, L. D. M. Miranda, G. Haack, R. Silva, J. B. Brask, and N. Brunner. "Markovian master equations for quantum thermal machines: local versus global approach". *New Journal of Physics*. **19**(12). 2017, p. 123037.

[8] S. Vinjanampathy and J. Anders. "Quantum thermodynamics". *Contemporary Physics*. **57**(4). 2016, pp. 545–579.

[9] O. Svelto and D. C. Hanna. *Principles of lasers*. Vol. 4. Springer, 1998.

[10] J. T. Verdeyen. "Laser electronics". *Laser electronics/2nd edition*. 1989.

[11] R. E. Sonntag and G. J. Van Wylen. *Introduction to thermodynamics: classical and statistical*. Wiley New York, 1991.

[12] K. Huang. "Statistical mechanics, john wily & sons". *New York*. 1963, p. 10.

[13] R. Kosloff. "Quantum thermodynamics: A dynamical viewpoint". *Entropy*. **15**(6). 2013, pp. 2100–2128.

[14] T. Yan and K. Gottfried. *Quantum mechanics: fundamentals*. 2013.

[15] S. Haroche and J.-M. Raimond. *Exploring the quantum: atoms, cavities, and photons*. Oxford university press, 2006.

[16] D. Manzano. "A short introduction to the Lindblad master equation". *AIP Advances*. **10**(2). 2020, p. 025106. ISSN: 2158-3226.
DOI: 10.1063/1.5115323.

[17] R. Alicki and R. Kosloff. "Introduction to quantum thermodynamics: History and prospects". *Thermodynamics in the Quantum Regime*. Springer, 2018, pp. 1–33.

[18] S. Krämer, D. Plankensteiner, L. Ostermann, and H. Ritsch. "QuantumOptics. jl: A Julia framework for simulating open quantum systems". *Computer Physics Communications*. **227**. 2018, pp. 109–116.

[19] M. Fox. *Quantum optics: an introduction.* Vol. 15. OUP Oxford, 2006.

[20] S.-W. Li, M. B. Kim, G. S. Agarwal, and M. O. Scully. "Quantum statistics of a single-atom Scovil–Schulz-DuBois heat engine". *Physical Review A.* **96**(6). 2017, p. 063806.

Eidesstattliche Erklärung

Ich erkläre hiermit an Eides statt durch meine eigenhändige Unterschrift, dass ich die vorliegende Arbeit selbständig verfasst und keine anderen als die angegebenen Quellen und Hilfsmittel verwendet habe. Alle Stellen, die wörtlich oder inhaltlich den angegebenen Quellen entnommen wurden, sind als solche kenntlich gemacht.

Ich erkläre mich mit der Archivierung der vorliegenden Bachelorarbeit einverstanden.

....
Markus Dannemüller   Datum